NOTE

Assessing the relative accuracy of coral heights reconstructed from drones and structure from motion photogrammetry on coral reefs

E. Casella[1] · P. Lewin[1] · M. Ghilardi[1,2] · A. Rovere[3] · S. Bejarano[1]

Abstract Low-altitude high-resolution aerial photographs allow for the reconstruction of structural properties of shallow coral reefs and the quantification of their topographic complexity. This study shows the scope and limitations of two-media (air/water) Structure from Motion—Multi-View Stereo reconstruction method using drone aerial photographs to reconstruct coral height. We apply this method in nine different sites covering a total area of about 7000 m^2, and we examine the suitability of the method to obtain topographic complexity estimates (i.e., seafloor rugosity). A simple refraction correction and survey design allowed reaching a root mean square error of 0.1 m for the generated digital models of the seafloor (without the refraction correction the root mean square error was 0.2 m). We find that the complexity of the seafloor extracted from the drone digital models is slightly underestimated compared to the one measured with a traditional in situ survey method.

Keywords UAS · Drone · SfM-MVS · Shallow coral reef · Structural complexity · Chain and tape

Topic Editor Stuart Sandin

✉ E. Casella
elisacasellaphd@gmail.com

[1] ZMT, Leibniz Centre for Tropical Marine Research, Bremen, Germany

[2] Faculty of Biology and Chemistry, University of Bremen, Bremen, Germany

[3] MARUM, University of Bremen, Bremen, Germany

Introduction

Centimeter-resolution 3D (or 2.5D) mapping of very shallow (< 3 m depth) coral reefs is a challenge. Large corals reach up to mean sea level, thus preventing the navigation of vessels carrying ship-borne echo sounders and limiting divers' access to continuous top-view data. Airborne bathymetric active light detection and ranging (LiDAR) can overcome these limitations and provide continuous sub-meter resolution data with a vertical accuracy in the range of 1–2 dm for shallow-water coral reefs (Collin et al. 2018). However, LIDAR surveys are costly and likely unjustified for small areas, and they allow for minimal flexibility in the survey design.

In the last years, Unoccupied Aircraft System (UAS, also called drones) started to be regarded as a third-generation source of remote sensing data (Simic Milas et al. 2018), providing scientists new and accessible tools to explore the Earth surface (e.g., Casella et al. 2020; Dugdale et al. 2019; Castellanos-Galindo et al. 2019; Mlambo et al. 2017) and allowing significant scientific advancement (e.g., Ramanathan et al. 2007). UAS regulation that has hindered early scientific uses of UASs (Coops et al. 2019) is now moving forward. The European Union represents an example where the different UAS regulations of each EU country are now unified under a common and simplified regulation (EU 2018/1139 and implementing acts). A review of worldwide UAS regulations is presented by Stöcker et al. (2017). Concurrently, advances in computer vision algorithms (Anderson et al. 2019) and hardware (e.g., GPU) facilitated the use of photogrammetry through Structure from Motion (SfM) (Ullman 1979) and Multi-View Stereo reconstruction (MVS) methods (Scharstein and Szeliski 2002). Today, SfM-MVS methods represent a core data capture and analysis approach widely used by

earth and environmental scientists (Anderson et al. 2019; James et al. 2019).

These technological and scientific advances facilitate the collection of centimeter-resolution continuous top-view data of shallow reefs at relatively low cost with more flexibility in the survey plan or experimental design (e.g., Casella et al., 2017). Although these are clear advantages for coral reef mapping and research, few studies surveying coral reefs with UASs and SfM-MVS exist compared to studies on terrestrial ecosystems (David et al. 2021; Fallati et al. 2020; Levy et al. 2018; Casella et al. 2017). The refraction of light by water, which causes features on the seafloor to appear shallower than they are may have led to this discrepancy because it introduces more significant errors than on-land environments. In addition, turbidity, water surface roughness, and the maximum depth for light penetration represent additional error sources (Joyce et al. 2018; Woodget et al. 2015). Some possible solutions to reduce the effect of the refraction of light on UAS SfM-MVS derived data exist or are being developed (Agrafiotis et al. 2020; Shintani and Fonstad 2017; Dietrich 2017; Ye et al. 2016; Woodget et al. 2015; Maas 2015).

This study aims to investigate the relative accuracy of coral height reconstruction of two-media (air/water) SfM-MVS datasets derived from low-altitude UAS flights on shallow coral reefs (< 3 m depth). Rather then focusing on the geographic accuracy, our goal is to answer the question: "how accurately (relative accuracy) can we reconstruct coral height?". Working on a selected area in Palau (western Micronesia), we assess the relative accuracy of selected coral heights in the reconstructed Digital Surface Models (DSMs) using 51 independent measurements (IMs), and we calculate 2D and 3D seafloor rugosity, comparing it with the results of the traditional "chain and tape" in situ method (Risk 1972; McCormick 1994).

Methods

Field surveys were conducted in the Palau Archipelago, western Micronesia (Fig. 1a), between November 2019 and February 2020. We focused on nine shallow reefs located in Nikko Bay (7°20′13.1″N 134°29′07.4″E) (Fig. 1a), a semi-enclosed bay characterized by a maze of shallow-water channels, separated by shallow sills emerging during spring low tides (Golbuu et al. 2016). These reefs are of particular ecological value and scientific interest because of their unusually warm and acidic waters and counter-intuitively high coral coverage and diversity (Golbuu et al. 2016; Kurihara et al. 2021). They are also particularly amenable to UAS surveys because they are sheltered from the wind by steep rocky cliffs and have low hydrodynamic influence from the adjacent ocean (Golbuu et al. 2016).

Therefore, study sites have periods of low hydrodynamic and wave motion and relatively low suspended sediment concentration. The surveys were carried out with calm winds (less than 2 km h^{-1}).

A consumer-grade UAS (DJI Phantom-4 Pro) was used to collect 980 near nadir photographs, covering a total area of 6830 m^2 across all reef sites. The Phantom-4 Pro has an integrated RGB sensor 1'' CMOS (effective pixel: 20 M), a focal length of 9 mm, and a resolution of 5472 × 3648 pixels (as per technical specifications: dji.com/phantom-4pro). Nine different flights were programmed to survey the sites at an altitude of 10 m (see Supplementary Table). The DJI Ground Station Pro app (dji.com/de/ground-station-pro) was used to program the UAS flights so that each flight resulted in a 90% forward and lateral overlap. Two types of markers were placed on the seafloor of each site before the flights (Fig. 1c, d): ground control points (GCPs) and scale bars (SBs). A total of 45 30 × 30 cm bright-colored towels and 29 50 cm-long steel bars covered by bright-colored tape were used as GCPs and SBs, respectively. The geographic position of GCPs was collected using a handheld GNSS receiver (Garmin eTrex® 10) with a horizontal accuracy in the order of meters, and their vertical position (local depth) was measured with a hand-held Hondex PS-7 dive sonar with reference to the local water level at the time of measurement. The position of GCPs and the length of SBs were used to scale the point cloud generated during the SfM-MVS process. The position of GCPs was also used to georeference the point cloud, optimize the image alignment, and minimize the sum of the re-projection error and the georeferencing error of the estimated internal camera parameters and point cloud in the SfM-MVS method.

The acquired photographs, GCPs, and scale bars were used as inputs in the SfM-MVS method through Agisoft Metashape 1.6.2 (agisoft.com) to reconstruct a 3D model of the scene captured by aerial photographs. Specifically, DSMs and orthomosaics of each reef were reconstructed (Fig. 1d, e). For a comprehensive description of the SfM-MVS method, the reader is referred to Westoby et al. (2012) and Carrivick et al. (2016).

To validate the DSMs, IMs were collected at each site. Over the entire study area, the height of 51 corals was measured with a meter rod in situ to the nearest centimeter. The IMs are represented mostly by conspicuous massive corals with one side almost perpendicular to the seafloor, ending on a sand patch, and were easily recognized and measured in the orthomosaics. The approximate geographic location of the 51 corals was recorded with the same GNSS receiver used for GCPs. In case the corals used as IM were not entirely conspicuous within the reef landscape in the proximity of the collected GNSS point,
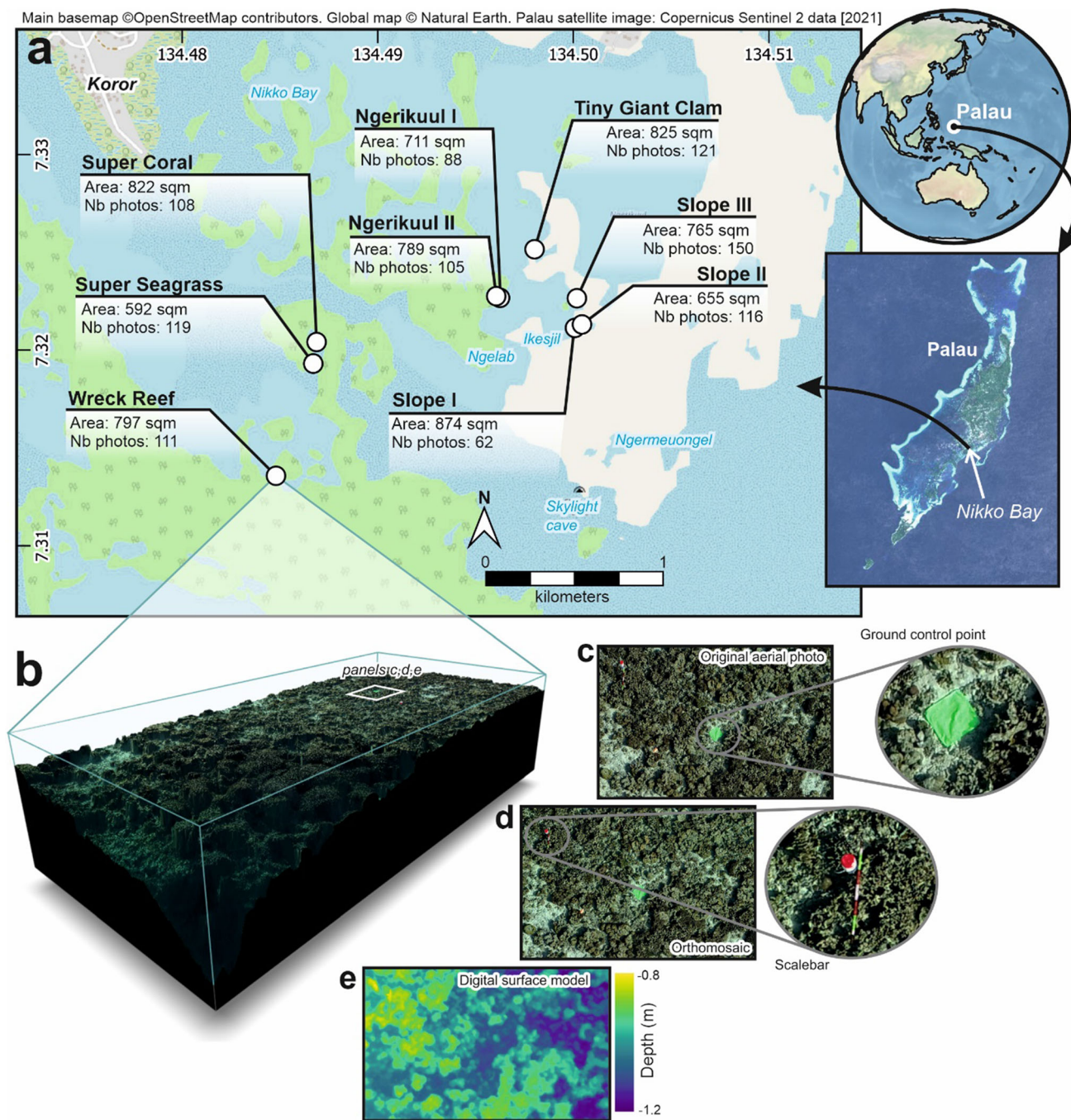
Fig. 1 **a** Location of the survey sites in the Palau Archipelago. The insets show the location of Palau in the Pacific Ocean and the location of Nikko Bay in Palau; **b** 3D rendering of DSM and Orthomosaic from one of the sites made with the R package *"Rayshader"* (github.com/tylermorganwall/rayshader/); **c** Detail of one original aerial photograph; **d** and **e** Orthomosaic and digital surface model (of the same area as **c**) obtained from the SfM-MVS workflow, respectively. Examples of ground control point and scale bar are also shown in the insets

markers were placed near the corals to help their identification on the orthomosaics.

Due to the refraction of light at the interface air–water, depths appear shallower than they are. This effect should be accounted for, given that the original DSMs calculated by Agisoft Metashape are not corrected for refraction. To account for this effect, we used a simple correction (Dietrich 2017; Woodget et al. 2015; Westaway et al. 2000) based upon Snell's Law, which governs the refraction of light between two media and is expressed as:

$$n_1 sin(i) = n_2 sin(r) \qquad (1)$$

where n_1 is the refractive index of seawater in Palau, n_2 is the refractive index of air (1.0), i is the angle of incident light rays originating below the water surface, r is the angle of refracted light rays above the water surface (Fig. 2a).

The simplified version of Snell's Law uses the small-angle approximation, with which, for angles less than ca. 15° (ca. 0.25 rad):

$$sin(i) \approx tan(i) \approx \frac{x}{h} \qquad sin(r) \approx tan(r) \approx \frac{x}{h_a}, \qquad (2)$$

where h is the real depth, h_a is the apparent depth, and x is the distance between the intersection of the light ray with the sea surface and the point (Fig. 2a). This simplifies Eq. 1 to:

$$h = n_1 h_a. \qquad (3)$$

Since photos were acquired near nadir, the effect of refraction introduced by oblique viewing angles (off-nadir camera) is minimized. The refractive index is remarkably constant (Westaway et al. 2001). Minor variations depend on salinity, temperature, pressure, and wavelength (Austin and Halikas 1976). Based on the ranges of sea surface temperature and salinity in Palau (i.e., from 27 to 30.5 °C and 33.6 ± 0.5 psu, as per Conroy et al. 2017, Colin 2018), the refractive index for the study area has a value between 1.341 and 1.342 (Austin and Halikas 1976).

Topographic complexity was measured in situ along ten 20 m line transects using the traditional "chain and tape" method (Risk 1972; McCormick 1994) (Fig. 3a). A ∼ 0.2 cm bead ball chain was used. Given that each of these transects' starting and ending points were marked

in situ and are visible in the orthomosaics, it was possible to identify the position of almost the same transects (digital transects) on the refraction-corrected DSMs. Using Quantum GIS (version 3.16, QGIS.org, 2022), we quantified the linear rugosity (hereafter referred to as 2D rugosity) and the area rugosity (hereafter referred to as 3D rugosity) on the digital transects. Both in situ and 2D rugosity were calculated by dividing the length obtained following the shape of the terrain (i.e., bottom profile) with the linear distance (for our case, it is 20 m for each transect) between starting and ending points of the transect (Fig. 3a). The 3D rugosity was calculated using the same method but buffering the digital transect line 0.5 m on each side. In this case, the 3D surface (DSM) was divided by 20 m² (as the transect swath is 20 m long and 1 m wide). The closer the rugosity is to zero, the flatter is the terrain.

Results and discussion

The average resolution of the reconstructed orthomosaics and DSMs is 0.3 cm pix⁻¹ and 0.6 cm pix⁻¹, respectively. The average XY and Z errors on GCPs are 120 and 7 cm, respectively (see Supplementary Table and Report). Comparing the coral heights measured in situ (IMs) with those estimated using corrected and uncorrected DSMs, we find that using refraction-corrected DSMs reduces the root-mean-square error (RMSE) from 21 to 10 cm (Fig. 2b). The variation across sites is reported in the Supplementary Table. It is noteworthy that coral height is still underestimated in the corrected DSMs, albeit slightly. Compared to
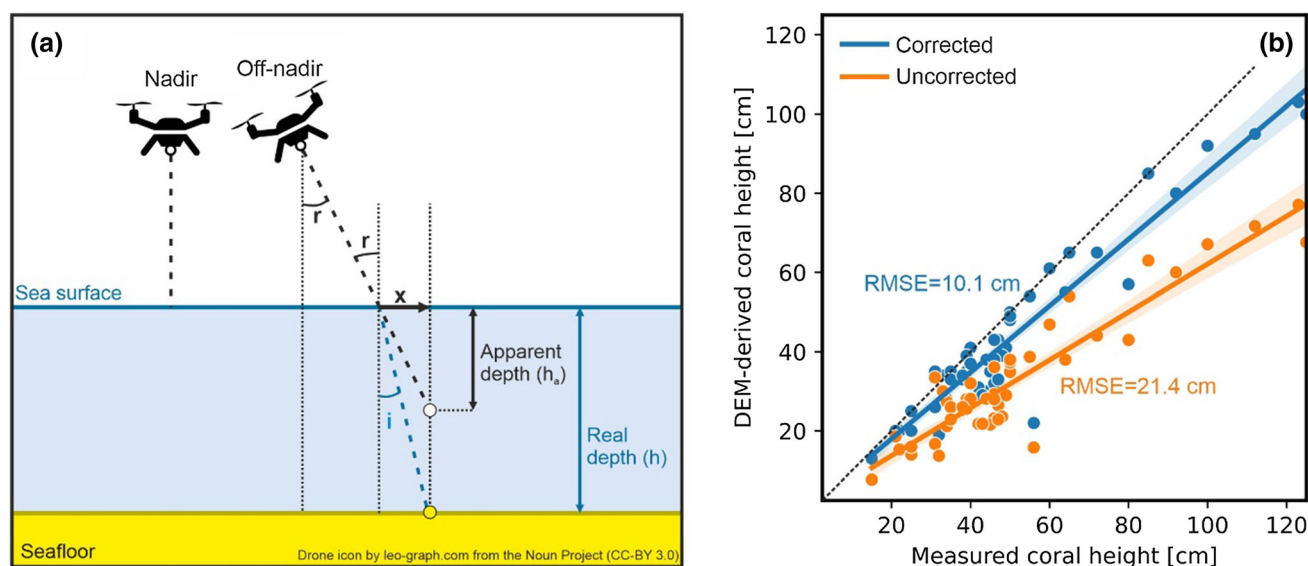

Fig. 2 a Incident (i) and refracted (r) angles of the light ray (modified and adapted from Dietrich 2017; Woodget et al. 2015; Westaway et al. 2001); b Comparison between coral heights measured in situ and derived from refraction-corrected and uncorrected DSMs, for the 51 IMs in the study area. The dotted line on panel b shows a 1:1 correlation for reference
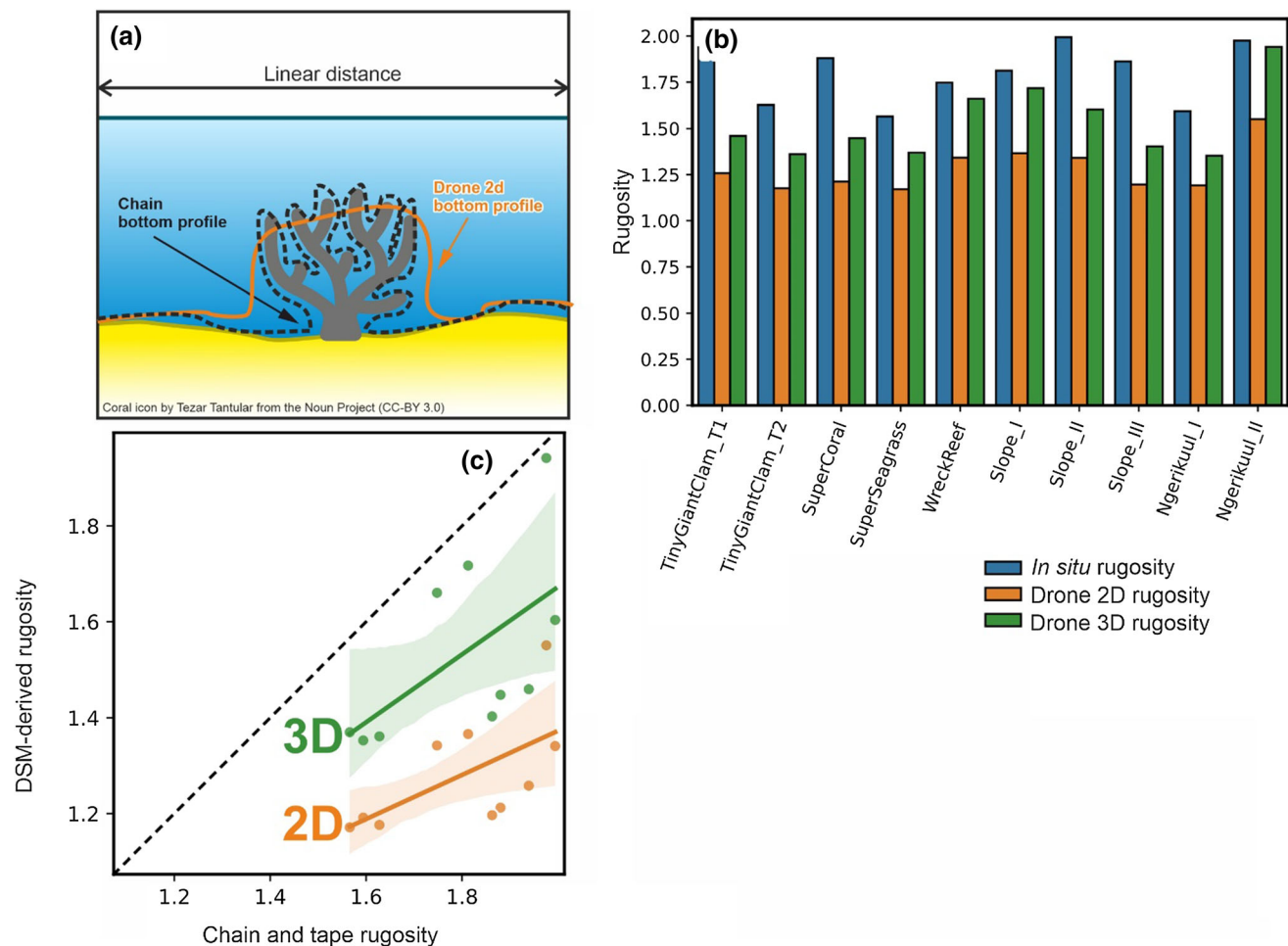
Fig. 3 **a** Difference between in situ vs 2D rugosity; **b** Histograms representing reef rugosity as calculated in situ and from the DSMs (2D and 3D rugosity, see text); **c** linear relationships (fitted lines and confidence intervals) between the in situ rugosity and the DSM-derived rugosity (both 2D and 3D). The dotted line shows the 1:1 relationship for reference

uncorrected DSMs, which underestimate coral heights by 35% (this is due to the current limits of the method and the propagation of DSM errors, James et al. 2017), corrected DSMs underestimate them by 13%. We argue that such correction is effective when flying at a low altitude (e.g. 10 m) and collecting near-nadir images on very shallow areas. The incident and refracted angles of the light ray should be very small ($< 15°$) for the correction equations to hold true. Surveys conducted under different settings are unlikely to benefit from this simple refraction correction. Yet, very promising methods to correct the refraction of light on SfM-MVS derived data are being implemented and will hopefully become widely available (e.g., Agrafiotis et al. 2020).

The UAS-derived 2D rugosity was always lower than the in situ rugosity (Fig. 3b). This can be explained by: (i) the underestimation of digital coral heights, (ii) the different resolution of the chain and the digital transects (~ 0.2 cm and ~ 0.6 cm respectively), (iii) the fact that

the chain goes in small interstices that are not solved in the 3D model (e.g. those characterizing branching corals). Also, the UAS-derived 3D rugosity which includes a larger area has slightly lower values than the in situ rugosity (Fig. 3b, c).

In this study, rather than concentrating on the absolute depth of the reconstructed seascapes, we focus on the reconstruction of selected coral heights within the scene, which in turn defines reef topographic complexity. Reconstructing shallow-water seascapes from UAS photographs is challenging and is subject to higher uncertainties in the final products than those usually attained with SfM-MVS topographic reconstructions of terrestrial habitats. This is mainly because light rays travel through two media (air–water), and many conditions need to be met (e.g., atmospheric conditions, sea state, light penetration, and water depth, nadir data collection) to achieve accuracies in the order of centimeters. Within this study, the conditions of all nine sites on different dates allowed for

their 3D reconstruction. Such conditions are not unique, as shown in Fallati et al. (2020) who successfully monitored biannual changes in substrate type and reef complexity in the Maldives at a maximum water depth of 1.5 m using a DJI Phantom 4 and SfM-MVS methods analogous to the ones used here, albeit without the refraction correction applied in this study.

Topographic complexity is one of the most striking features of coral-dominated reefs. Complex topographies offer ample space for reef-associated organisms to settle, feed, and shelter from predators and water motion, thus typically supporting higher levels of biodiversity (Graham and Nash 2013). Central to maintaining complex topographies are processes that sustain net accretion and cementation of the reefs' carbonate framework, which underpins the functionality of reefs as barriers protecting shorelines from wave-driven erosion (Perry et al. 2008). Measuring topographic complexity on reefs provides information on their capacity to support biodiversity and ecosystem services. With increasingly common and prolonged marine heatwaves causing severe coral mortality and leading to the reduction of architectural complexity (Oliver et al. 2018), it is urgent to optimize methods to quantify topographic complexity accurately. The simple method proposed here provides information on topographic complexity with a vertical accuracy of 0.1 m using a 3D model of the seafloor derived from UAS data. Further refinements and improvements will be possible once corrections of refraction of light and additional error sources (e.g., water surface roughness, light penetration) are developed and integrated into the SfM-MVS method.

References

Agrafiotis P, Karantzalos K, Georgopoulos A, Skarlatos D (2020) Correcting image refraction: towards accurate aerial image-based bathymetry mapping in shallow waters. Remote Sensing. https://doi.org/10.3390/rs12020322

Anderson K, Westoby MJ, James MR (2019) Low-budget topographic surveying comes of age: Structure from motion photogrammetry in geography and the geosciences. Progress in Physical: Geography Earth and Environment. https://doi.org/10.1177/0309133319837454

Austin RW, Halikas G (1976). The index of refraction of seawater. University of California, San Diego Visibility Laboratory of the Scripps Institution of Oceanography, Lajolla, California. SIO Ref. No. 76–1. https://escholarship.org/content/qt8px2019m/qt8px2019m.pdf

Carrivick JL, Smith MW, Quincey DJ (2016) Structure from motion in the Geosciences. Wiley, Hoboken

Casella E, Collin A, Harris D, Ferse S, Bejarano S, Parravicini V, Hench JL, Rovere A (2017) Mapping coral reefs using consumer-grade drones and structure from motion photogrammetry techniques. Coral Reefs. https://doi.org/10.1007/s00338-016-1522-0

Casella E, Drechsel J, Winter C, Benninghoff M, Rovere A (2020) Accuracy of sand beach topography surveying by drones and photogrammetry. Geo-Mar Lett. https://doi.org/10.1007/s00367-020-00638-8

Castellanos-Galindo GA, Casella E, Mejía-Rentería JC, Rovere A (2019) Habitat mapping of remote coasts: Evaluating the usefulness of lightweight unmanned aerial vehicles for conservation and monitoring. Biol Cons 239:108282

Colin PL (2018) Ocean warming and the reefs of Palau. Oceanography 31(2):126–135

Collin A, Ramambason C, Pastol Y, Casella E, Rovere A, Thiault L, Espiau B, Nakamura N, Siu G, Hench J, Schmitt R, Holbrook S, Troyer M, Davies N (2018) Very high resolution mapping of coral reef state using airborne bathymetric LiDAR surface-intensity and drone imagery. Int J Remote Sens. https://doi.org/10.1080/01431161.2018.1500072

Conroy JL, Thompson DM, Cobb KM, Noone D, Rea S, Legrande AN (2017) Spatiotemporal variability in the δ18O-salinity relationship of seawater across the tropical Pacific Ocean. Paleoceanography 32(5):484–497

Coops NC, Goodbody TR, Cao L (2019) Four steps to extend drone use in research. Nature 572:433–435

David CG, Kohl N, Casella E, Rovere A, Ballesteros P, Schlurmann T (2021) Structure-from-Motion on shallow reefs and beaches:

potential and limitations of consumer-grade drones to reconstruct topography and bathymetry. Coral Reefs. https://doi.org/10.1007/s00338-021-02088-9

Dietrich JT (2017) Bathymetric Structure-from-Motion: extracting shallow stream bathymetry from multi-view stereo photogrammetry. Earth Surf Proc Land 42(2):355–364. https://doi.org/10.1002/esp.4060

Dugdale SJ, Kelleher CA, Malcolm IA, Caldwell S, Hannah DM (2019) Assessing the potential of drone-based thermal infrared imagery for quantifying river temperature heterogeneity. Hydrol Process 33(7):1152–1163

Fallati L, Saponari L, Savini A, Marchese F, Corselli C, Galli P (2020) Multi-Temporal UAV Data and object-based image analysis (OBIA) for estimation of substrate changes in a post-bleaching scenario on a maldivian reef. Remote Sensing 12(13):2093

Golbuu Y, Gouezo M, Kurihara H, Rehm L, Wolanski E (2016) Long-term isolation and local adaptation in Palau's Nikko Bay help corals thrive in acidic waters. Coral Reefs 35(3):909–918

Graham NAJ, Nash KL (2013) The importance of structural complexity in coral reef ecosystems. Coral Reefs 32(2):315–326

James MR, Robson S, d'Oleire-Oltmanns S, Niethammer U (2017) Optimising UAV topographic surveys processed with structure-from-motion: ground control quality, quantity and bundle adjustment. Geomorphology 280:51–66

James MR, Chandler JH, Eltner A, Fraser C, Miller PE, Mills JP, Noble T, Robson S, Lane SN (2019) Guidelines on the use of structure-from-motion photogrammetry in geomorphic research. Earth Surf Proc Land 44(10):2081–2084

Joyce KE, Duce S, Leahy SM, Leon J, Maier SW (2018) Principles and practice of acquiring drone-based image data in marine environments. Mar Freshw Res 70(7):952–963

Kurihara H, Watanabe A, Tsugi A, Mimura I, Hongo C, Kawai T, Reimer JD, Kimoto K, Gouezo M, Golbuu Y (2021) Potential local adaptation of corals at acidified and warmed Nikko Bay. Palau Scientific Reports 11(1):1–10

Levy J, Hunter C, Lukacazyk T, Franklin EC (2018) Assessing the spatial distribution of coral bleaching using small unmanned aerial systems. Coral Reefs 37(2):373–387

Maas HG (2015) On the accuracy potential in underwater/multimedia photogrammetry. Sensors 15(8):18140–18152

McCormick MI (1994) Comparison of field methods for measuring surface topography and their associations with a tropical reef fish assemblage. Mar Ecol Prog Ser 112:87–96

Mlambo R, Woodhouse IH, Gerard F, Anderson K (2017) Structure from motion (SfM) photogrammetry with drone data: a low cost method for monitoring greenhouse gas emissions from forests in developing countries. Forests 8(3):68

Oliver EC, Donat MG, Burrows MT, Moore PJ, Smale DA, Alexander LV, Benthuysen JA, Feng M, Gupta AS, Hobday AJ, Holbrook NJ, Perkins-Kirkpatrick SE, Scannell HA, Straub SC, Wernberg T (2018) Longer and more frequent marine heatwaves over the past century. Nat Commun 9(1):1–12

Perry CT, Spencer T, Kench PS (2008) Carbonate budgets and reef production states: a geomorphic perspective on the ecological phase-shift concept. Coral Reefs 27(4):853–866

QGIS.org, 2022. QGIS Geographic Information System. QGIS Association. http://www.qgis.org. Accessed 5 Apr 2022

Ramanathan V, Ramana MV, Roberts G, Kim D, Corrigan C, Chung C, Winker D (2007) Warming trends in Asia amplified by brown cloud solar absorption. Nature 448(7153):575

Risk MJ (1972) Fish diversity on a coral reef in the Virgin Islands. Atoll Res Bull 193:1–6

Scharstein D, Szeliski R (2002) A taxonomy and evaluation of dense two-frame stereo correspondence algorithms. Int J Comput Vision 47:7–42

Shintani C, Fonstad MA (2017) Comparing remote-sensing techniques collecting bathymetric data from a gravel-bed river. Int J Remote Sens 38(8–10):2883–2902. https://doi.org/10.1080/01431161.2017.1280636

Simic Milas A, Cracknell AP, Warner TA (2018) Drones–the third generation source of remote sensing data. Int J Remote Sens 39:7125–7137

Stöcker C, Bennett R, Nex F, Gerke M, Zevenbergen J (2017) Review of the current state of UAV regulations. Remote Sensing 9(5):459

Ullman S (1979) The interpretation of structure from motion. Proc R Soc Lond B Biol Sci 203(1153):405–426

Westaway RM, Lane SN, Hicks DM (2000) The development of an automated correction procedure for digital photogrammetry for the study of wide, shallow, gravel-bed rivers. Earth Surface Processes and Landforms: the Journal of the British Geomorphological Research Group 25(2):209–226

Westaway RM, Lane SN, Hicks DM (2001) Remote sensing of clear-water, shallow, gravel-bed rivers using digital photogrammetry. Photogramm Eng Remote Sens 67(11):1271–1282

Westoby MJ, Brasington J, Glasser NF, Hambrey MJ, Reynolds JM (2012) 'Structure-from-Motion' photogrammetry: a low-cost, effective tool for geoscience applications. Geomorphology 179:300–314

Woodget AS, Carbonneau PE, Visser F, Maddock IP (2015) Quantifying submerged fluvial topography using hyperspatial resolution UAS imagery and structure from motion photogrammetry. Earth Surf Proc Land 40(1):47–64

Ye D, Liao M, Nan A, Wang E, Zhou G (2016) Research on reef bathymetric survey of UAV stereopair based on two-medium photogrammetry. ISPRS-International Archives of the Photogrammetry, Remote Sensing and Spatial Information Sciences 41:407–412